Self-Tuning Pump Operation Mode For Fluid Storages To Increase Energy Efficiency

Thomas Hieninger (M.Sc.), Prof. Dr.-Ing. Ronald Schmidt-Vollus
Nuremberg Campus of Technology, Fuerther Straße 264b, D-90429 Nuremberg
Nuremberg Institute of Technology, Kesslerplatz 12, D-90489 Nuremberg
thomas.hieninger@th-nuernberg.de

ABSTRACT

This contribution deals with a self-tuning strategy for centrifugal pumps running fluid storages to decrease energy demand. The results are based on a MATLAB/Simulink model of a pump system, which is explained and verified. To analyse the energy demand and time for filling processes and to examine the applicability of the self-tuning strategy three possible systems and different filling strategies are regarded. Based on the most efficient strategy a self-tuning program was developed. For this program, convenient starting conditions and target values for constant or variable outflow are described. Thus, this optimisation strategy can be used as an on-line tuning program, which is simple to implement in running pump storage systems. The tuning strategy is tested with a genetic algorithm and a Nelder-Mead algorithm. Finally, a self-tuning program for fixed time operation mode is shown.

Keywords**:** Self-tuning, Pump Operation, Energy Efficiency

1 INTRODUCTION AND RELATED WORK

According to estimates the electrical energy demand of pumps in industrial nations is about 20 %, moreover, water distribution systems need up to seven percent of electrical power [1, 2]. Essential components in such plants are pump driven water or fluid reservoirs, which represent a significant amount of energy demand in water distribution systems or in other industries. There are several publications describing optimal operating strategies for tank filling processes to decrease dissipated energy. In [3, 4, 5] the optimal rotational speed respective flowrate is shown in dependence of the static head. Therefore, guided by the storage level a variable speed drive control can be implemented and used to minimize the energy demand. If the filling strategy should be realized, an inadequate knowledge about system characteristics leads to problems and inaccuracies. For those reasons, a self-tuning mode is useful to optimise the pump system [6]. In this paper, a mathematical model is used for simulating different systems. These systems are optimised with a self-tuning algorithm during filling operations with variable outflow in view of a decreasing energy demand and filling time.

2 PUMP SYSTEM MODEL

MATLAB/Simulink is used to model the pump systems in order to optimise the control strategy for reducing energy demand. The basic structure is shown Figure 1. The motor and pump characteristics are adapted from a test rig and steady plus transient states are verified in this section.

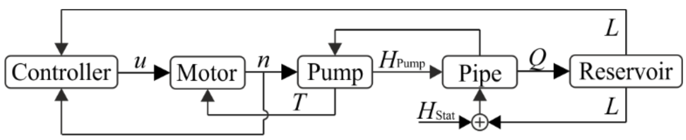

Figure 1. Signal flow diagram for a modelled pumped storage.

The controller produces an output value u to the motor subsystem. With the current torque T the system commits the rotational speed n to the pump and with the current flow rate Q the total pump head H_{Pump} is calculated. In combination with filling level L and the static head H_{Stat} the flow rate is given by the pipe subsystem, which is used to fill the fluid storage.

2.1 MOTOR INCLUDING CONTROL UNIT

By means of the setpoint and the actual value a PID transfer function calculates the controller output. For the sake of convenience, no DC converter between the PID controller and the motor is realized, so the controller output corresponds to the armature voltage U_{A} of the modelled DC motor.

The DC drive is modelled in its basic structure as a standard linear model. To emulate nonlinear behaviour additional losses T_{Loss} like friction torque and nonlinear motor constants $k_{1/2}\phi$ are included. Both can nearly be described in dependence of the actual motor load (see Figure 2a). The nonlinear transfer function of second order is given in Equation 1, where the armature resistance R_{A}, the inductivity L_{A} and the mechanical inertia J are implemented as proportional gain factors. The static behaviour is given in Figure 2b and 2c.

$$\ddot{n}2\pi J\frac{L_A}{R_A} + \dot{n}2\pi J + n\frac{k_1\phi \cdot k_2\phi}{R_A} = U_A\frac{k_2\phi}{R_A} - (T_{Loss} + T_{Load}) - (\dot{T}_{Loss} + \dot{T}_{Load})\frac{L_A}{R_A} \qquad (1)$$

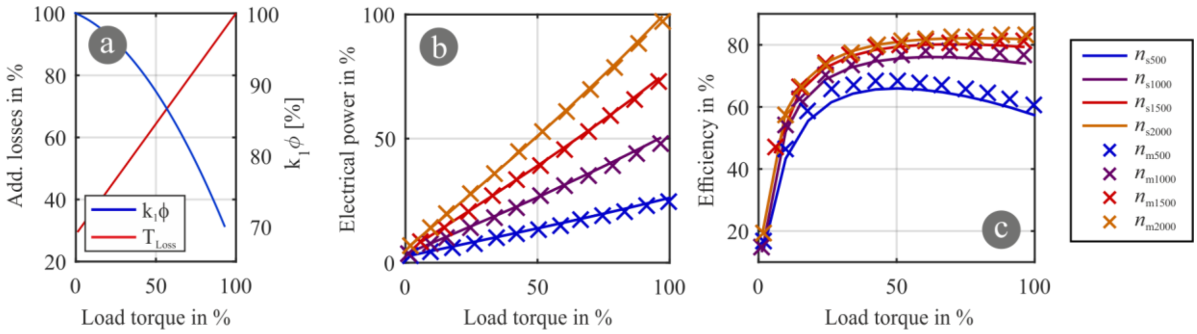

Figure 2. a) Additional losses and $k_1\phi$ in dependence of the load. Characteristic motor curves with different rotational speeds for b) electrical power and c) efficiency. Index "s" figures the simulated curves and "m" the measured values.

2.2 PUMP

The pump is modelled as nonlinear gain functions for the head H_{Pump} and the torque T_{Pump}, which are based on the affinity laws without time behaviour (see Figure 3a and 3b). The head and torque are described by polynomial functions of fifth order (Equation 2 and 3). Considering deviations of the affinity laws linear correction functions using the coefficients $k_{\mathrm{H}1,2}$ and $k_{\mathrm{T}1,2}$ are added (see Figure 4a). The coefficients are determined by the method of least squares.

$$H_{Pump} = A_1Q^5\left(\frac{n_n}{n}\right)^3 + A_2Q^4\left(\frac{n_n}{n}\right)^2 + A_3Q^3\frac{n_n}{n} + A_4Q^2 + A_5Q\frac{n}{n_n} + A_6\left(\frac{n}{n_n}\right)^2 + k_{H1}n + k_{H2} \qquad (2)$$

$$T_{Pump} = B_1Q^5\left(\frac{n_n}{n}\right)^3 + B_2Q^4\left(\frac{n_n}{n}\right)^2 + B_3Q^3\frac{n_n}{n} + B_4Q^2 + B_5Q\frac{n}{n_n} + B_6\left(\frac{n}{n_n}\right)^2 + k_{T1}n + k_{T2} \qquad (3)$$

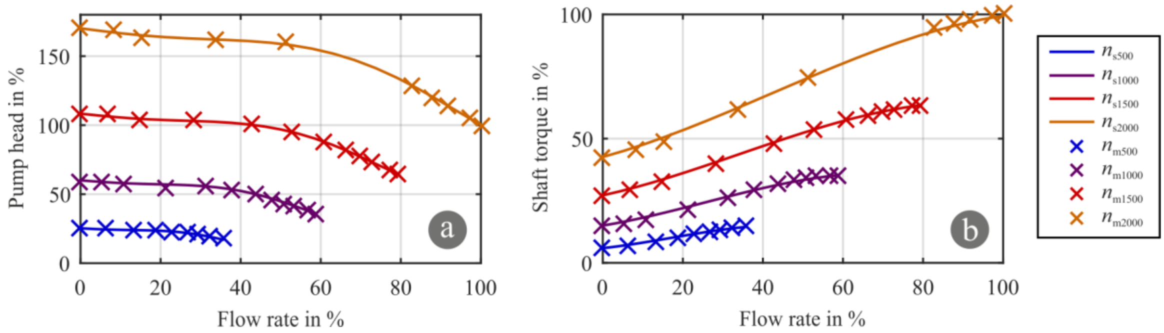

Figure 3: a) Fitted head flow characteristic curve. b) Fitted torque flow characteristic curve.

2.3 Pipe and Storage

The pipe including fluid storage can be described with a nonlinear transfer function of second order, using storage and pipeline cross sections A_{Stor} and A_{Pipe}, gravity g, pipe length l_{Pipe} and H_{Stat} to determine the storage level L. The transfer function can be written as:

$$\ddot{Q} + 2\frac{A_{Pipe}g}{l_{Pipe}}k_{Pipe}\dot{Q}Q + \frac{A_{Pipe}g}{A_{Stor}l_{Pipe}}Q = \frac{A_{Pipe}g}{l_{Pipe}}\dot{H}_{Pump} - \frac{A_{Pipe}g}{l_{Pipe}}(\dot{L}) \quad (4)$$

$$k_{Pipe} = \frac{1}{2\,A_{Pipe}^2\,g}\left(\lambda \cdot \frac{l_{Pipe}\sqrt{\pi}}{2\sqrt{A_{Pipe}}} + \zeta\right) \quad (5)$$

Whereby k_{Pipe} is a function to describe the coherence between the flow rate and the dynamic pressure drop. The loss coefficient ζ characterises components in the pipe system and the friction factor λ losses due to pipe friction, depending on the Reynolds number Re. To calculate λ for turbulent flow regime directly, the approximation (Equation 7) according to Haaland [7] is used.

$Re \le 2{,}000$: $$\lambda = \frac{64}{Re} \quad (6)$$

$Re \ge 3{,}000$: $$\lambda = 1/\left(-1.8\,ln\left(\frac{6.9}{Re} + \left(\frac{r}{3700 \cdot d_{Pipe}}\right)^{10/9}\right)\right)^2 \quad (7)$$

In the transition flow regime (2,000 < Re < 3,000) a linear interpolation between both is adapted, the factor $r = 0.1$ mm describes the roughness in steel tubes.

2.4 Model Verification

To verify the model, step responses for the flow rate are recorded in a test rig. At constant rotational speeds, a valve is opened instantly. In Figure 4b the measured and simulated transient flow behaviours are illustrated. The simulated step responses using the fitted affinity laws have a higher consistency with the recorded values, especially at lower speeds compared to the plan solution based on the affinity laws without correction functions.

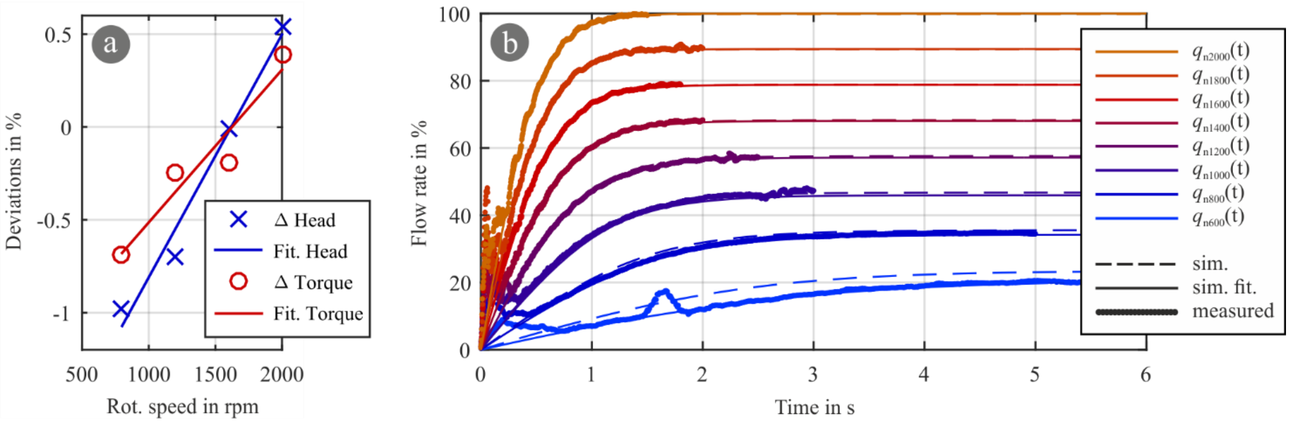

Figure 4: Fitted functions for head and torque deviations. b) Transient behaviour of a water column - measured values, simulated values with and without fitted functions.

3 FILLING STRATEGIES

First, three different pipe and storage systems are presented. In the second part, these systems are applied to several filling modes and compared to each other to create an adequate control function. Finally, two process acceleration possibilities are shown and evaluated.

3.1 REGARDED SYSTEMS

To generate universal optimisation strategies different pump systems are modelled (see Table 1). In dependence of the pump head with the best efficiency point (BEP) at the rotational speed of $n =$ 1,800 rpm the pipe length, the static head and the filling level are modified. Thus, adequate reference points are created and the following results are compared to the BEP. The resistance coefficient is given as $\zeta = 5$. The rotational speed is limited between 500 rpm $\leq n \leq$ 2,000 rpm.

Table 1. Different system variants.

Variety	Length [m]	Pipe Diameter [m]	Static Head [m]	Filling Level [m]
V1	590	0.100	25	10
V2	63	0.075	20	15
V3	590	0.100	1	34

3.2 LEVEL GUIDED CONTROL

In general, three control strategies can be adapted and optimised to fill a fluid storage (see Figure 5a):

- $n_{\mathrm{C,Opt}}$: optimal filling with constant rotational speed
- $Q_{\mathrm{C,Opt}}$: optimal filling with constant flow rate
- $n_{\mathrm{L,Opt}}$: optimal filling with level guided rotational speed control (LGC)

The LGC is directly determined by the actual total static head, consisting of the fill level and the static head of the installation (see Figure 5b).

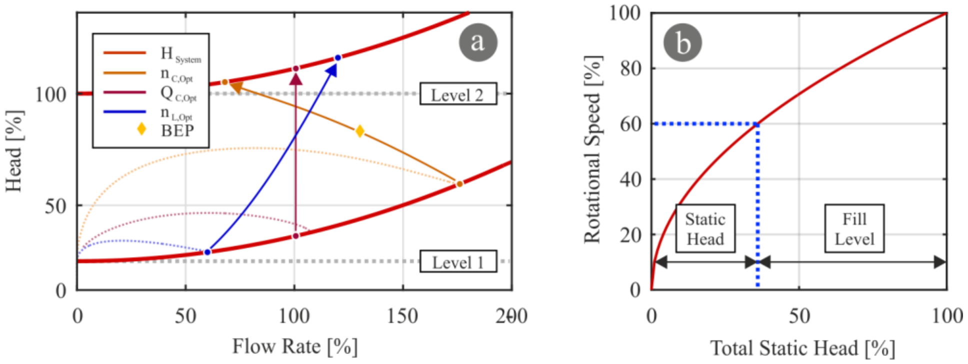

Figure 5: a) Different filling strategies. b) LGC function.

The energy saving potential for these strategies are validated to choose a suitable method for self-tuning processes. Additional to this, six different possibilities to create an appropriate head speed function for the LGC are checked (see Equation 9). All operation modes are optimised by the Nelder-Mead method, where p, a, r are model parameters fitted by using the starting values a_0 and r_0 (see Section 4.2).

$$H_{S,tot} = H_{Stat} + L \tag{8}$$

$$n_L = \left\{ n_L | n_L \to min(E) \right\} \text{ with}$$
$$n_L \in M_n = \{ \left(p + r \cdot H_{S,tot}{}^{a}\right)_1, \left(r \cdot H_{S,tot}{}^{a}\right)_2, \left(p + r \cdot H_{S,tot}{}^{a_0}\right)_3, \tag{9}$$
$$\left(p + r_0 \cdot H_{S,tot}{}^{a}\right)_4, \left(r_0 \cdot H_{S,tot}{}^{a}\right)_5, \left(r \cdot H_{S,tot}{}^{a_0}\right)_6 \}$$

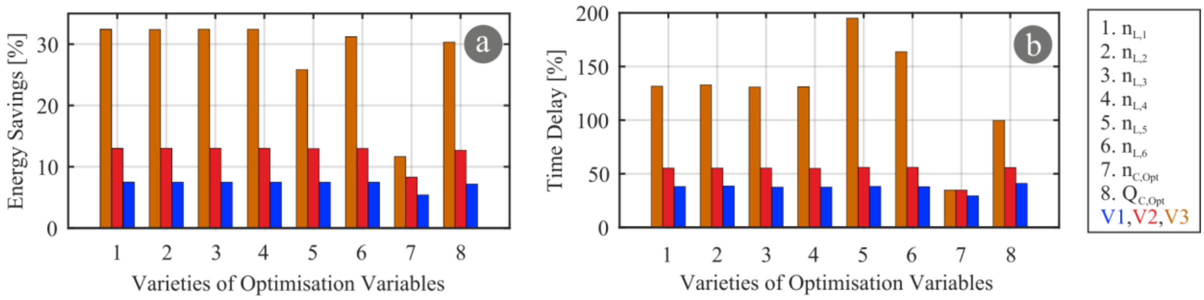

Figure 6: a) Energy savings and b) time delay for varieties of optimisation variables and for system varieties V1, V2, V3 compared to the BEP.

In Figure 6a the resulting energy savings for the systems V1, V2 and V3 are shown, whereby for all systems the LGC varieties one to four reach the highest energy saving potentials. To reduce calculation costs for optimisation a simple model with two parameters is preferable. Because of suitable and available starting values for a_0 and r_0 (see Section 4.2) variety two is selected for further optimisation steps. All strategies exhibit time delay (see Figure 6b) induced by lower rotational speeds. This effect is treated in the next section.

3.3 TIME REGARDED FILLING

The settings for an energy saving LGC leads to an increase of filling time. Due to that a time fitting function is adapted to compensate this delay. In this section two possibilities are compared with each other to achieve a minimal filling work (Equation 10).

$$n_L^* = \left\{ n_L' | n_L' \rightarrow min(E) \right\} \text{ with } n_L' \in \ M_{nL} = \{(k + n_L)_1, (k \cdot n_L)_2\} \tag{10}$$

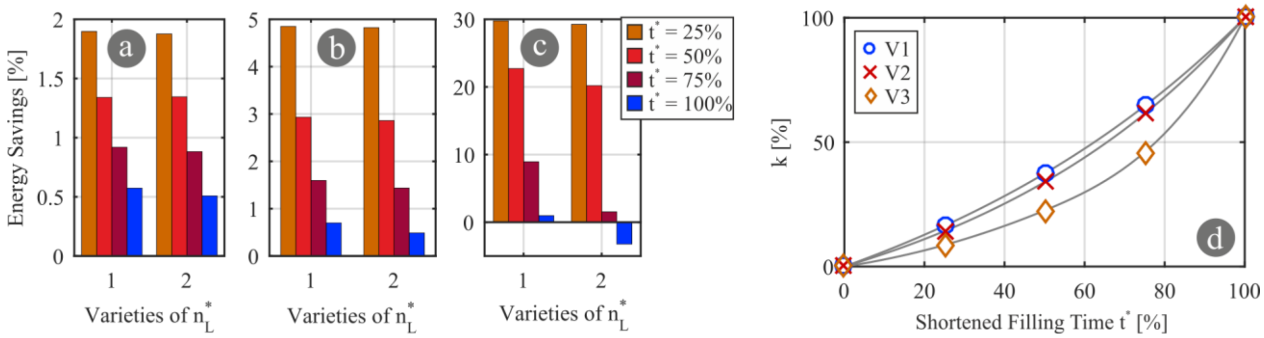

Figure 7: Energy savings for a) V1 b) V2 c) V3 with different t. d) Coherence between t* and k.*

Different fixed times t^* between filling times with $n = 1{,}800\ rpm$ and with LGC are considered. To validate t^* the required energy is compared with the demand using an adapted fixed speed for the same filling time. In Figure 7a-c can be seen, that for all three cases (V1-V3) variety one reaches higher energy saving potential than variety two, especially in combination with V3. The coherence between the shortened filling time and the acceleration factor k for variety one is shown in Figure 7d. To build a function, which gives a good reproduction of this coherence, a polynomial of fourth order in combination with minimum six measuring points is adapted. This function is used in the time tuning algorithm (see Section 4.5).

4 SELF-TUNING PROGRAMMES

In the following section, a tuning program based on the LGC is presented and applied. For variation of the tuning values a and r the energy demand is examined. Further, a target value for varying outflow rates is presented an analysed. These are implemented in two optimisation algorithms, which are compared to each other. Finally, a fixed time mode for constant outflows is shown.

4.1 Optimisation Problem

In Figure 8 energy per filling in dependence of a and r are shown. Here, dark blue marks the minimum and yellow the maximum energy demand. The white area is a dead zone where filling is not possible due to insufficient rotational speed. Figure 8a-c displays $\tilde{E}_{\text{Spec}}$ for V1-V3 (see Section 4.3), whereas Figure 8d shows E per filling for V1. In compare to Figure 8a, the area and the located optima are similar (see Section 4.3). For V1 and V2 the optimisation problem is easy to solve with single global minima, whereas V3 have two local minima.

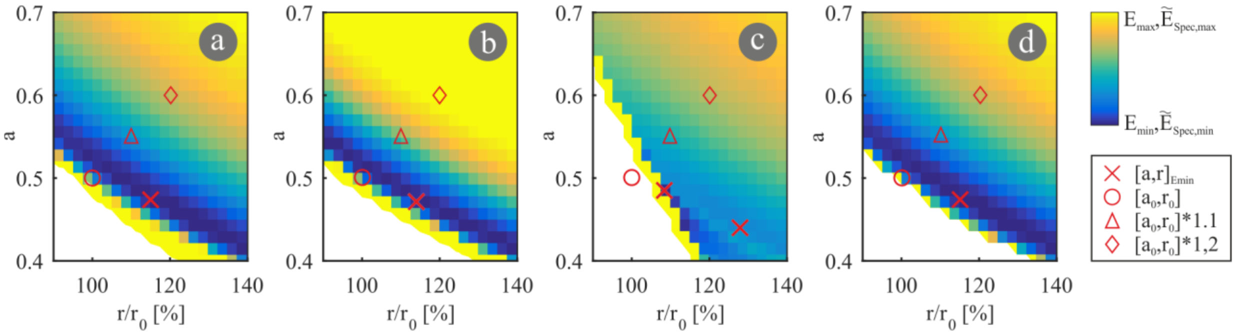

Figure 8: $\tilde{E}_{Spec}$ for a) V1, b) V2, c) V3. d) E for V1.

4.2 Starting Values

To run an efficient self-tuning operation, suitable starting values are necessary. Using the affinity laws in combination with the BEP the starting values r_0 and a_0 can be generated by comparing coefficients:

$$n = \frac{n_C}{H_{C,BEP}^{0.5}} \cdot h^{0.5} \triangleq r_0 \cdot h^{a_0} \tag{11}$$

In Figure 8 the starting values are illustrated, whereby in V1 and V2 the values are next to good solutions, in V3 the starting values are outside of operation range. To create proper values, they are amplified by 10 % and 20 % and checked on their iteration efficiency in Section 4.4.

4.3 Target Value

In order to minimise the energy requirement during filling operations an appropriate objective function is needed. Varying outflow from storages causes variances in total pump work per filling. Due to this, the pump work is not a suitable target value for optimisation purposes (see Figure 9b). A convenient value to compare filling processes is a modification of the specific energy (Equation 12), which describes the integrated electrical power P_{Elec} divided through the integrated flow rate during one filling process.

$$\tilde{E}_{Spec} = \int_{t(Level\ 1)}^{t(Level\ 2)} P_{Elect}(t) \cdot dt \,/ \int_{t(Level\ 1)}^{t(Level\ 2)} Q_{Pump}(t) \cdot dt \tag{12}$$

It also can be expressed as total work per filled volume, so the following coherence is given:

$$min(E) \triangleq min(\tilde{E}_{Spec}) \tag{13}$$

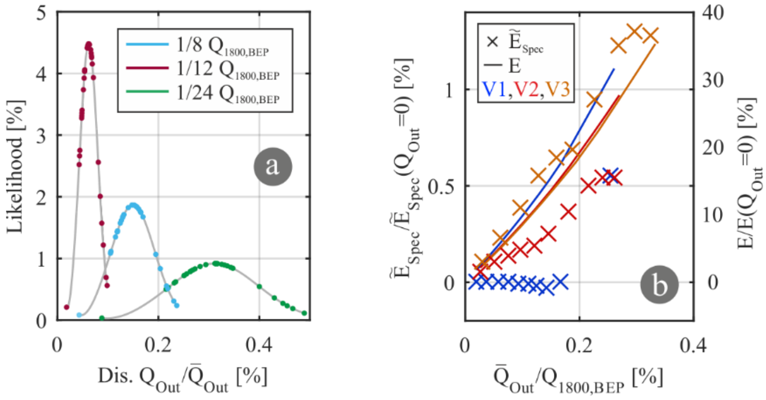

Figure 9: a) Distribution of the $\bar{Q}_{out}$ per filling V1 (1.800 rpm, 30 iterations). b) Deviations of $\tilde{E}_{Spec}$ and E fo a varying Q_{out}

To validate the use of $\tilde{E}_{\mathrm{Spec}}$ a varying outflow is implemented in the model, which consists of two varying parameters. The first one q_{Random} is a time depending random value, that modifies the outflow during the filling process. The second one q_{Gain} randomly changes the amplifying of the first one each filling process. In order to avoid too many on/off switches the maximum mean gain value is set to: $\bar{q}_{\mathrm{Gain,max}} \approx 1/8\, Q_{1800,\mathrm{BEP}}$. The resulting discharge is dampened with a time constant $T = 100$s. The transfer function is given in Equation 14.

$$T \cdot \dot{Q}_{Out} + Q_{Out}(t) = q_{Random}(t) \cdot q_{Gain} \tag{14}$$

The distribution of Q_{Out} with three mean gain factors is shown for V1 in Figure 9a.

In Figure 9b $\tilde{E}_{\text{Spec}}$ is compared to E for all system varieties V1, V2 and V3. In relation to a filling process with no discharge, $\tilde{E}_{\text{Spec}}$ still displays deviations per filling, even so less than 30 times in compare to E. For outflow rates below 20 % of $Q_{1800,\text{BEP}}$ the maximum deviation amount to 0.7 percent. Hence, $\tilde{E}_{\text{Spec}}$ can be used as suitable target value with varying outflows.

4.4 SELF-TUNING OF ENERGY EFFICIENT OPERATION MODE

For simple optimisation problems (see Figure 8) two standard optimisation algorithms are applied in this contribution and integrated in the tuning algorithm. The first one is the Nelder-Mead algorithm (NM) and the second one a genetic algorithm (GA) with population size ten. The iterations for different starting values are shown in Figure 10a-c for GA and in Figure 10d-f for NM. It can be recognised, that the NM converges with far less iteration steps than the GA. The optimisation using starting values with no gain reaches the optima at first, except for V3. With a gain of 20 % the optimisation takes the longest and the rotational speed exceeds its limit (section 3.1). Thus, a recommended sensible gain for all three systems is 10 %.

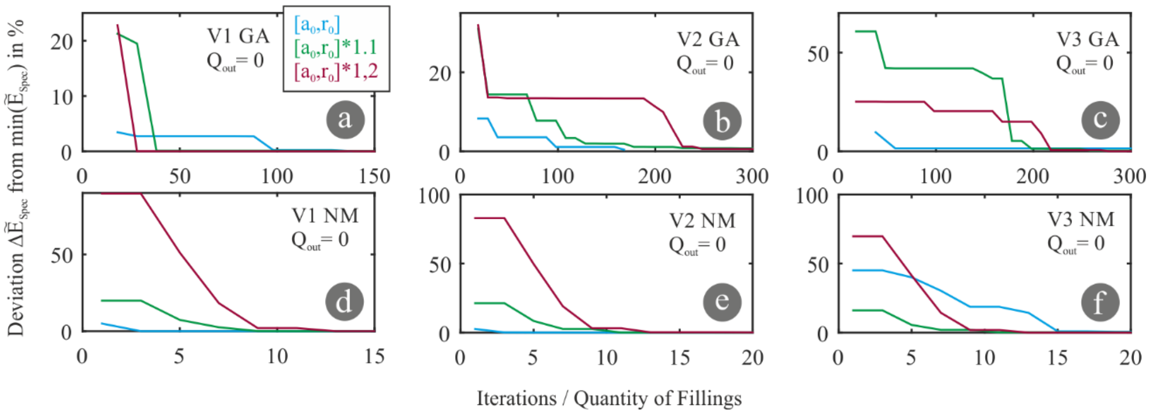

Figure 10: Deviations from the optimum in dependence of the iterations for GA and NM.

The optimisation for varying outflow rates using starting values with 10 % gain is exposed in Figure 11. Here, optimisations using NM with three distributions of $\bar{Q}_{\text{out}}$ (see Figure 9a) are applied. For V1 and V2 the target value converges to the minimum below 20 fillings. For V3 $\bar{Q}_{\text{out}}$ reveals a bigger influence on the iteration steps, where $\bar{q}_{\text{Gain,max}}$ shows the slowest approach and even does not reach the same minimum like the NM in V1 and V2.

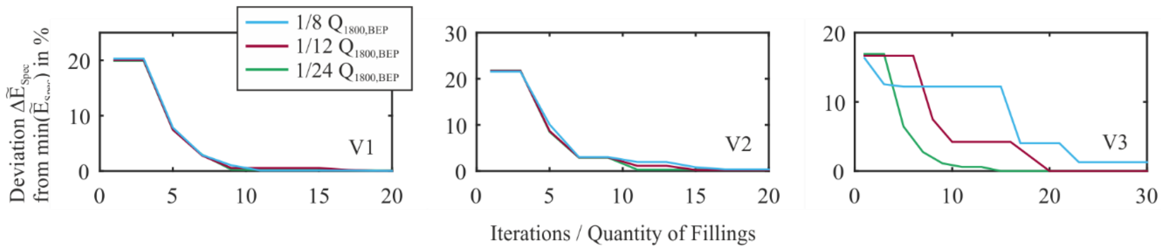

Figure 11: Deviations from the optimum in dependence of iteration steps with varying discharge.

4.5 Self-Tuning of a fixed Time Operation Mode

After generating the settings for the LGC, the function for the acceleration factor $k = f(t^*)$ can be created using a polynomial with order $m = 4$. For rotational speeds between $n_{\max,\mathrm{LGC}} \leq n_i \leq n_{\max,\mathrm{limit}}$ six points of support are generated and the resulting filling times are recorded. The coefficients A_j are determined by the method of least squares, whereby $A = 0$ with $j = m + 1$ and the starting values are set to $A_{0,j} = 0$. In Figure 12 the deviations for the simulated time in dependence of the ascertained function $k = f(t^*)$ are figured out. The differences between filling times for V1 and V2 are almost zero percent. V3 shows small variances up to about 0.08 percent. So, with the help of this tuning mode a predetermined filling time is attainable for constant outflow rates.

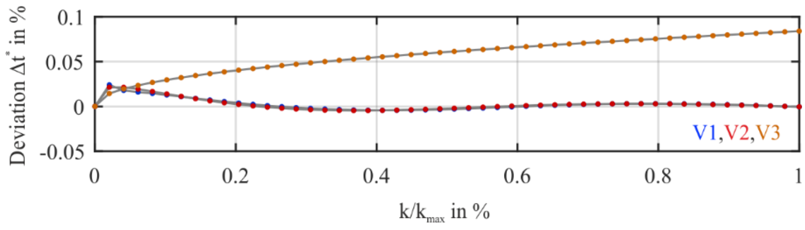

Figure 12: time deviations in dependence of the acceleration factor k

5 CONCLUSIONS

In this contribution, the saving potential for pump driven storages have been shown. Depending of the system, savings about 30 % are possible using LGC. A sensible level speed function has been developed, which can be integrated in a control unit. Additionally, an implementable function has been generated to accelerate the filling process. The optimisation problem has been analysed and thus, suitable starting values for LGC are presented, which can be used in storage systems driven by centrifugal pumps. Further, a target value has been shown, that demonstrates good properties to increase energy efficiency in combination with constant or varying discharge. Therefore, this value allows an on-line tuning mode during filling processes. To suggest an adequate optimisation algorithm, two standard algorithms have been checked on their iteration efficiency. It has been concluded that the NM algorithm approaches faster to good operation mode. It also has been shown that for varying outflow rates this tuning algorithm benefits short iteration steps. Finally, for constant outflow rates a self-tuning program to compensate the time delay has been suggested.

References

[1] Hydraulic Institute, Europump and the US Department of Energy, "Variable speed pumping - a guide to successful applications. Executive summary", 2004.

[2] Coelho et al., "Efficiency achievement in water supply systems — A review", *Renewable and Sustainable Energy Reviews*, pp. 58 – 84, 2014.

[3] Santos et al., "Optimized strategies for fluid transport and reservoirs management", *Revista Minerva Pesquisa e Technologia*, pp. 91 – 98, 2005.

[4] Ahonen et al., "Energy efficiency optimizing speed control method for reservoir pumping applications", *Energy Efficiency*, pp. 117 – 128, 2015.

[5] Lindstadt et al., "Optimal control of pump rotational speed in filling and emptying a reservoir: minimum energy consumption with fixed time", *Energy Efficiency*, 2016.

[6] Hieninger et al., "Process optimisation through auto-tuning of pump systems — an efficiency boosting opportunity", *Process Technology & Components*, pp 4 – 10, 2017.

[7] Haaland, "Simple and Explicit Formulas for the Friction Factor in Turbulent Flow", *Journal of Fluids Engineering*, pp 89 – 90, 1983.